Asphaltene Adsorption onto an Iron Surface: Combined Near-Infrared (NIR), Raman, and AFM Study of the Kinetics, Thermodynamics, and Layer Structure

ARTICLE *in* ENERGY & FUELS · DECEMBER 2010

Impact Factor: 2.79 · DOI: 10.1021/ef100779a

6 AUTHORS, INCLUDING:

Johannes Stadler
AAC Infotray AG
19 PUBLICATIONS **684** CITATIONS
SEE PROFILE

Ekaterina Lomakina-Rumyantseva
ETH Zurich
20 PUBLICATIONS **780** CITATIONS
SEE PROFILE

Renato Zenobi
ETH Zurich
459 PUBLICATIONS **13,157** CITATIONS
SEE PROFILE

Energy Fuels **2011,** *25,* 189–196 · DOI:10.1021/ef100779a
Published on Web 12/03/2010

energy&fuels
article

Asphaltene Adsorption onto an Iron Surface: Combined Near-Infrared (NIR), Raman, and AFM Study of the Kinetics, Thermodynamics, and Layer Structure

Roman M. Balabin,[†] Rustem Z. Syunyaev,[‡] Thomas Schmid,[†] Johannes Stadler,[†] Ekaterina I. Lomakina,[§] and Renato Zenobi*[,†]

[†]*Department of Chemistry and Applied Biosciences, ETH Zurich, 8093 Zurich, Switzerland,* [‡]*Gubkin Russian State University of Oil and Gas, 119991 Moscow, Russia, and* [§]*Faculty of Computational Mathematics and Cybernetics, Lomonosov Moscow State University, 119992 Moscow, Russia*

Received June 21, 2010. Revised Manuscript Received November 12, 2010

A combination of near-infrared (NIR) spectroscopy, Raman microscopy, and atomic force microscopy (AFM) was used to analyze the adsorption behavior of petroleum macromolecules (asphaltenes) on an iron (Fe) surface. A partial least-squares (PLS/PLSR) regression method was used for determining the concentration from NIR spectroscopic data. A Langmuir model was used to fit the experimental data. Effective kinetic and thermodynamic parameters (Gibbs energy of adsorption, adsorption/desorption rate constant, maximal adsorbed mass density) of asphaltenes adsorbed from benzene solution were evaluated: the maximum adsorbed mass density (Γ_{max}) was found to be 4.90 ± 0.07 mg m^{-2}; the adsorption constant (K) was found to be 0.084 ± 0.007 L mg^{-1}; and a value of 34.3 ± 0.2 kJ mol^{-1} was calculated for the effective Gibbs energy of absorption ($-\Delta G_{ads}$). The structure of the adsorbed layer was also analyzed by AFM. Asphaltenes were found to form aggregates on Fe surface with an average size of a few hundred nanometers. The notion of a nonuniform distribution of crude oil macromolecules adsorbed on metal surfaces was experimentally confirmed.

1. Introduction

Asphaltenes are commonly described as a class of petroleum molecules that are insoluble in normal alkanes (*n*-pentane or *n*-heptane) but soluble in aromatics such as benzene or toluene.[1,2] They are considered to be the most polar fraction of crude oil.[3,4] Asphaltenes are a complex mixture of macromolecules with molecular weights (MW) that range from 500 up to 100,000 Da according to different authors and methods.[5,6] Their interfacial activity is attributed to the presence of different functional groups (e.g., nitrogen and oxygen containing groups)[7] although their nature and their role in the interfacial activity is not fully understood.[2,4] Other parameters, such as the amount of native petroleum resins, can also be of great importance for asphaltene interfacial properties.[1,4,8,9]

Asphaltenes and resins are the main elements ("core") of petroleum's colloid structure.[4,8,10] Asphaltenes can undergo phase separation and deposition due to changes in temperature, pressure, and/or solution composition[2,11] during production, transportation, and during the refining processes. Asphaltene deposition on metal surfaces of the transportation/production equipment is undesirable and both preventive and treatment methods can be extremely expensive.[12] Selection of an appropriate mitigation technique, such as a suitable surfactant or coating material for metal surfaces exposed to asphaltenes, are typically based on an empirical approach owing to the limited understanding of the asphaltene−metal interactions.[2,13,14] A fundamental understanding of these interactions (their thermodynamics and kinetics) will lead to a deeper understanding of the adsorption phenomena which play a critical role in the deposition process. Thus, investigations that yield information on the asphaltene adsorption behavior can greatly help the modern petroleum industry (from crude oil production and transportation to petroleum refining).

A number of studies have focused on asphaltene/resin adsorption onto different surfaces. A lot of attention has been

*To whom correspondence should be addressed. Telephone: +41-44-632-4376. E-mail: zenobi@org.chem.ethz.ch.

(1) Speight, J. G. *The Chemistry and Technology of Petroleum*; CRC Press: Boca Raton, FL, 1999.
(2) Rudrake, A.; Karan, K.; Horton, J. H. *J. Colloid Interface Sci.* **2009**, *22*, 332.
(3) (a) Syunyaev, R. Z.; Balabin, R. M.; Akhatov, I. S.; Safieva, J. O. *Energy Fuels* **2009**, *23*, 1230. (b) Balabin, R. M.; Safieva, R. Z.; Lomakina, E. I. *Anal. Chim. Acta* **2010**, *671*, 27.
(4) (a) Mullins, O. C.; Sheu, E. Y.; Hammami, A.; Marshall, A. G. *Asphaltenes, Heavy Oils, and Petroleomics*, 1st ed.; Springer: New York, 2006. (b) Labrador, H.; Fernández, Y.; Tovar, J.; Muñoz, R.; Pereira, J. C. *Energy Fuels* **2007**, *21*, 1226. (c) Jouault, N.; Corvis, Y.; Cousin, F.; Jestin, J.; Barr, L. *Langmuir* **2009**, *25*, 3991.
(5) Groenzin, H.; Mullins, O. C. *Energy Fuels* **2000**, *14*, 677.
(6) Groenzin, H.; Mullins, O. C. *J. Phys. Chem. A* **1999**, *103*, 11237.
(7) Marczewski, A.; Szymula, A. *Colloids Surf. A* **2002**, *208*, 259.
(8) Syunyaev, R. Z.; Balabin, R. M. *J. Dispersion Sci. Technol.* **2007**, *28*, 419.
(9) Schorling, P. C.; Kessel, D. G.; Rahimian, I. *Colloids Surf., A* **1992**, *152*, 95–102.
(10) Fenistein, D.; Barré, L.; Broseta, D.; Espinat, D.; Livet, A.; Roux, J. N.; Scarsella, M. *Langmuir* **1998**, *14*, 1013–1020.
(11) Hammami, A.; Phelps, C.; Monger-McClure, T.; Little, M. *Energy Fuels* **2000**, *14*, 14.
(12) Ratulowski, J.; Hammami, A. 3rd International Symposium on Colloid Chemistry in Oil Production, Asphaltene and Wax Deposition, 1999, Mexico.
(13) Karan, K.; Hammami, A.; Flannery, M.; Stankiewicz, A. *Pet. Sci. Technol.* **2003**, *21*, 629.
(14) Balabin, R. M. *Chem. Phys.* **2008**, *352*, 267.

paid to liquid−liquid (first of all, water) interfaces,[15−20] minerals (quartz, kaolin, smectite, dolomite, mica, etc.),[3,21−25] and even asphaltene particles themselves.[26,27] The adsorption of asphaltenes on metal surfaces has been studied only a few times.[28−31] Alboudwarej et al.[29] have studied the adsorption of Athabasca and Cold Lake asphaltenes on stainless steel (304 L), iron, and aluminum powders using UV−vis spectrophotometry. The effects of resins, temperature, and *n*-heptane-to-toluene ratio were also investigated. In all cases, Langmuir isotherms were observed, indicating that asphaltenes saturated the surface area available for adsorption. The saturation adsorptions of the asphaltenes on metals (0.25−2.7 mg m^{-2}) were of the same order of magnitude as that on minerals.[21,23] No information about the kinetics was provided in that study.

The adsorption of asphaltenes and resins onto gold surfaces as a function of bulk concentration has been studied by Sjöblom and co-workers.[30] A quartz crystal microbalance method with dissipation measurements (QCM-D) was used. Their results showed that the adsorbed amount for resins from heptane corresponds to a rigidly attached monolayer. Asphaltenes adsorbed in large quantities and their mass and dissipation data demonstrated the presence of aggregates on the surface. The aggregates are firmly attached and cannot be removed by addition of resins. An adsorbed mass density up to 10 mg m^{-2} was reported.[30] No information about thermodynamic quantities (e.g., equilibrium constants) or kinetic parameters was provided.

In the study reported by Xie and Karan[31] results on the kinetics and thermodynamics of asphaltene adsorption from toluene−heptane and toluene−pentane solutions were presented. The kinetics of asphaltene adsorption on gold surface was investigated using a quartz crystal microbalance in a flow-cell system. The kinetics of adsorption was found to be relatively slow and did not achieve equilibrium even after 700 min. The asymptotic analyses indicated that the initial adsorption process is controlled by diffusion of asphaltenes from the bulk solution to the adsorption surface.[31]

In this study we show a kinetic and thermodynamic analysis of asphaltene adsorption onto an iron surface. The choice of iron as the adsorbent was determined by industrial demands, as gold surfaces are of no importance for petroleum production and transportation. The structure of the adsorbed layer is also shown and partly analyzed by force microscopy technique. The combination of near-infrared (NIR) spectroscopy, Raman microscopy, and atomic force microscopy (AFM) methods was found to produce consistent information about the asphaltene adsorption process, proving the applicability of Langmuir adsorption model for asphaltene adsorption.[32−56] We focus here on generalizing and comparing the kinetcs of adsorption.

2. Experimental Section

2.1. Near Infrared (NIR) Setup. The home-built near-infrared (NIR) setup consisted of a hermetic glass cell (15 × 10 × 5 cm) and three NIR optical fibers that were fixed at distances of 2.5, 7.5, and 12.5 cm from the top of the reservoir. Each fiber led to a separate homemade spectrometer. Such a configuration enabled us to monitor solution concentrations at three different heights, ensuring that no sedimentation or phase separation occurred during the adsorption process. It also increased the amount of signal (per time unit) by a factor of 3. Identical halogen incandescent lamps were used as light sources and identical silicon photodiodes were used as detectors in the Fourier transform near-infrared spectrometers (FT-NIR).

The spectral region of 9000−13000 cm^{-1} (1111−769 nm) was scanned with a resolution of 16 cm^{-1} (12 scans). See ref 3 for more details. A photometric accuracy of 0.022% (transmittance) was reached for a collection time of 1.3 s (excluding the time for FT analysis). The optical path was varied from 1 to 5 cm.

(15) Goual, L.; Horváth-Szabó, G.; Masliyah, J. H.; Xu, Z. *Langmuir* **2005**, *21*, 8278–8289.
(16) Spiecker, P. M.; Kilpatrick, P. K. *Langmuir* **2004**, *20*, 4022.
(17) Jestin, J.; Simon, S.; Zupancic, L.; Barré, L. *Langmuir* **2007**, *23*, 10471–10478.
(18) Acevedo, S.; Ranaudo, M.; Escobar, G.; Gutierrez, L.; Ortega, P. *Fuel* **1995**, *74*, 595.
(19) Jeribi, M.; Almir-Assad, B.; Langevin, D.; Henaut, I.; Argillier, J. *J. Colloid Interface Sci.* **2002**, *256*, 268.
(20) Gafonova, O. V.; Yarranton, H. W. *J. Colloid Interface Sci.* **2001**, *241*, 469–478.
(21) Mendoza de la Cruz, J. L.; Castellanos-Ramírez, I. V.; Ortiz-Tapia, A.; Buenrostro-González, E.; Durán-Valencia, C. A.; López-Ramírez, S. *Colloids Surf., A* **2009**, *340*, 149–154.
(22) Lopez-Linares, F.; Carbognani, L.; Sosa-Stull, C.; Pereira-Almao, P; Spencer, R. J. *Energy Fuels* **2009**, *23*, 1901–1908.
(23) Acevedo, S.; Ranaudo, M. A.; Garcia, C.; Castillo, J.; Fernandez, A. *Energy Fuels* **2003**, *17*, 257.
(24) Gonzalez, G.; Moreira, M. *Colloids Surf., A*. **1991**, *58*, 293.
(25) Balabin, R. M.; Syunyaev, R. Z. *J. Colloid Interface Sci.* **2008**, *318*, 167–174.
(26) León, O.; Contreras, E.; Rogel, E.; Dambakli, G.; Acevedo, S.; Carbognani, L.; Espidel, J. *Langmuir* **2002**, *18*, 5106–5112.
(27) León, O.; Rogel, E.; Urbina, A.; Andújar, A.; Lucas, A. *Langmuir* **1999**, *15*, 7653–7657.
(28) Abdallah, W. A.; Taylor, S. D. *J. Phys. Chem. C* **2008**, *112*, 18963.
(29) Alboudwarej, H.; Pole, D.; Svrcek, W. Y.; Yarranton, H. W. *Ind. Eng. Chem. Res.* **2005**, *44*, 5585–5592.
(30) Ekholm, P.; Blomberg, E.; Claesson, P.; Auflem, I. H.; Sjoblom, J.; Kornfeldt, A *J. Colloid Interface Sci.* **2002**, *247*, 342–350.
(31) Xie, K.; Karan, K. *Energy Fuels* **2005**, *19*, 1252–1260.
(32) Balabin, R. M.; Safieva, R. Z.; Lomakina, E. I. *Chemometr. Intell. Lab. Syst.* **2008**, *93*, 58.
(33) Balabin, R. M. *J. Chem. Phys.* **2008**, *129*, 164101.
(34) Hair, J. F.; Black, W. C.; Babin, B. J.; Anderson, R. E. *Multivariate Data Analysis*, 7th ed.; Prentice Hall: Upper Saddle River, NJ, 2009.
(35) Balabin, R. M.; Safieva, R. Z. *Fuel* **2008**, *87*, 1096.
(36) Balabin, R. M.; Safieva, R. Z.; Lomakina, E. I. *Chemometr. Intell. Lab. Syst.* **2007**, *88*, 183.
(37) Wold, S.; Trygg, J.; Berglund, A.; Antti, H. *Chemometr. Intell. Lab. Syst.* **2001**, *58*, 131–150.
(38) Hall, J. W.; McNeil, B.; Rollins, M. J.; Draper, I.; Thompson, B. G.; Macaloney, G. *Appl. Spectrosc.* **1996**, *50*, 1.
(39) (a) Balabin, R. M.; Safieva, R. Z. *J. Near Infrared Spec.* **2007**, *15*, 343. (b) Balabin, R. M.; Safieva, R. Z. *Fuel* **2008**, *87*, 2745.
(40) Burns, D. A.; Ciurczak, E. W. *Handbook of Near-Infrared Analysis*, 3rd ed.; CRC: Boca Raton, FL, 2007.
(41) (a) Balabin, R. M. *J. Phys. Chem. A* **2009**, *113*, 4910. (b) Balabin, R. M. *J. Phys. Chem. A* **2009**, *113*, 1012.
(42) Syunyaev, R. Z.; Balabin, R. M. *J. Dispersion Sci. Technol.* **2008**, *29*, 1505.
(43) Bouhadda, Y.; Bormann, D.; Sheu, E.; Bendedouch, D.; Krallafa, A.; Daaou, M. *Fuel* **2007**, *86*, 1855–1864.
(44) Chung, H.; Ku, M. S. *Appl. Spectrosc.* **2000**, *54*, 239.
(45) Bouhadda, Y.; Fergoug, T.; Sheu, E. Y.; Bendedouch, D.; Krallafa, A.; Bormann, D.; Boubguira, A. *Fuel* **2008**, *87*, 3481–3482.
(46) Standard deviation and confidence interval (95%) have been calculated by authors after digitization of plotted data from ref 29.
(47) Lide, D. R. *Handbook of Chemistry and Physics*, 85th ed.; CRC: Boca Raton, FL, 2004.
(48) Barr, L.; Simon, S.; Palermo, T. *Langmuir* **2008**, *24*, 3709–3717.
(49) Gawrys, K. L.; Blankenship, G. A.; Kilpatrick, P. K. *Langmuir* **2006**, *22*, 4487.
(50) Liu, J.; Zhang, L.; Xu, Z.; Masliyah, J. *Langmuir* **2006**, *22*, 1485.
(51) Zielinski, L.; Saha, I.; Freed, D. E.; Hurlimann, M. D. *Langmuir* **2010**, *26*, 5014.
(52) Somasundaran, P.; Krishnakumar, S. *Colloids Surf., A* **1997**, *123−124*, 491.
(53) Bruch, L. W.; Cole, M. W.; Zaremba, E. *Physical Adsorption: Forces and Phenomena*; Dover Publications, 2007.
(54) Acevedo, S.; Castillo, J.; Fernández, A.; Goncalves, S.; Ranaudo, M. A. *Energy Fuels* **1998**, *12*, 86.
(55) Wang, S.; Liu, J.; Zhang, L.; Xu, Z.; Masliyah, J. *Energy Fuels* **2009**, *23*, 862.
(56) Indo, K.; Ratulowski, J.; Dindoruk, B.; Gao, J.; Zuo, J.; Mullins, O. C. *Energy Fuels* **2009**, *23*, 4460.

The frequency region scanned combines the advantages (selectivity/chemical information content) of vibrational spectroscopy (overtones of fundamental bands are observed in NIR) with the technical simplicity and low cost of absorption spectroscopy in the visible range. For these reasons, NIR is an attractive technique for modern petroleum science and industry[3] when compared to other methods, such as ellipsometry or reflectivity measurements.[4] In particular, NIR spectroscopic measurements allow differentiation of chemical structures by their vibrational overtones,[3] a feature that is not found in reflectivity measurements, where all chemical substances can influence the observed signal change (e.g., refractive index change). For example, using NIR, one can estimate the parameters of the asphaltene adsorption process in the presence of petroleum resins and vice versa. The same is true for Raman spectroscopy, which directly probes the "fingerprint region" of the molecular systems under study.[42]

Up to 30 metal sheets (15 × 5 × 0.65 cm) were placed vertically inside the cell. A constant distance of 2.5 mm between sheets was used. A total iron surface area of 0.45 m^2 was exposed to asphaltene solution.

The setup was placed in a thermostat (T adjustable from −50 to 105 °C; ± 0.05 °C). Three background spectra (12 scans each) were measured every 30 min to eliminate possible fluctuations of the source intensities or other conditions. Three sample spectra (from the three spectrometers) were averaged after separate background correction. All solute spectra were evaluated as a difference between background-corrected sample and background-corrected solvent spectra. Correction for cell adsorption was also done (see ref 25 for details).

2.2. AFM/Raman Setup. An upright Raman microscope (NTEGRA Spectra, NT-MDT, Russia) was employed for Raman microscopy and AFM measurements. The system was equipped with an upright confocal laser microscope, an atomic force microscope (AFM), a white-light video microscope for rough observation and alignment of the sample, a photomultiplier tube (PMT) detector for confocal imaging, and a Raman spectrograph equipped with a charge-coupled device (CCD). It allowed simultaneous AFM and optical measurements on exactly the same part of transparent and opaque samples. All optical measurements were performed using a 100× long working-distance objective with a numerical aperture (NA) of 0.7 for both excitation and collection of the backscattered light from the sample. Two lasers, a red HeNe (632.8 nm, 5 mW at the sample) provided by Laser Drive, Inc. and a green DPSS (532 nm, 3−4 mW at the sample) provided by Changchun New Industries (CNI) Optoelectronics Tech. Co., Ltd. were used for Raman spectroscopy. Twenty-five points of each sample were scanned and the results of the best 15 (all inside $\pm 3\sigma$ interval) were averaged.

Unfortunately, Raman scattering itself cannot provide us with the concentration or mass density of asphaltenes on the surface. The signal is proportional to both the concentration and Raman cross-section, which is unknown. So, Raman adsorption data were normalized using one point−the adsorbed mass density at 60 min as obtained by NIR spectroscopy. The linearity of "spectrum integral intensity−asphaltene content" dependence proves the validity of this approach and invariability of Raman cross-section during adsorption process. Only the adsorbed amount (not adsorption constant or effective Gibbs free energy) is influenced by this normalization procedure.

An area of 5 × 5 μm (256 × 256 pixels) was scanned by AFM in tapping mode with a speed of 1 line per second. AdvancedTEC cantilevers (NANOSENSORS, Switzerland) with resonance frequencies in the 210−490 kHz range and force constants of 12−110 N m^{-1} were used. The sample was adsorbed for a given amount of time by putting asphaltene solution in contact with clean Fe surface. After the process termination the surface with asphaltenes was quickly washed with benzene to remove any sediment and dried under ambient conditions. The nonuniform structure revealed by AFM imaging (see below, Section 3.4) could be the result of the sample deposition technique (drying effects). AFM data taken directly in benzene liquid could in the future help to clarify this issue,[55] but a liquid cell is not available for our instrumentation. Aggregation can happen in solution or at the iron/mica surface.[3] In the latter case, the final result is representative of processes taking place at the liquid−solid interface.

Table 1. Crude Oil Properties (Information Provided by Moscow Refinery Laboratory (Moscow, Russia))

name		-	West-Siberian
source		-	Moscow refinery
density		kg m^{-3}	856.1
viscosity		cP	7.9
SARA composition[a]	saturates	% w/w	36.1
	aromatics	% w/w	39.2
	resins	% w/w	22.3
	asphaltenes	% w/w	2.5
fractional composition	≤200 °C	% w/w	29.2
	≤350 °C	% w/w	62.1

[a] Measured by authors.

Table 2. Elemental Analysis of Petroleum Asphaltenes (in % w/w)

carbon	hydrogen	nitrogen	sulfur
87.3	7.2	2.2	2.1

2.3. Materials. *Crude Oil*. A mixture of West-Siberian crude oils (Russia) was used for asphaltene extraction. The sample was obtained from Moscow petroleum refinery (Moscow, Russia). The properties of the crude oil are given in Table 1. Note that exactly the same crude oil was used for petroleum resins extraction for NIR adsorption analysis.[25]

Asphaltenes. The asphaltenes were extracted from the crude oil (Table 1) using the following method.[25] The oil cut above 200 °C was mixed with petroleum ether (40−70 °C) in a 1:50 ratio (v/v). After short stirring at room temperature, the system was left for sedimentation (24 h). After settling, the sediment was filtered through filter paper (0.45 μm) at vacuum (100 mmHg). The sediment was washed with the same petroleum ether. The element analysis (Nitromatic 500 plus sulfur coulometric analyzer) of the asphaltenes is reported in Table 2. The asphaltenes were stored at −18 °C in vacuum-sealed ampules under argon (Ar) atmosphere. A solid-state asphaltene Raman spectrum is shown in Figure 1. The two modes (G and D1) characteristic for the natural poorly organized carbonaceous materials and for most commercial graphite (microcrystalline graphite) are easily seen.[43] The D1 peak arises from the in-plane defects and the heteroatoms that initiate breathing vibration modes of the sp^2 atoms in the rings.[43,45] The G mode corresponds to the stretching vibration of the sp^2 carbon atoms in the aromatic hexagonal sheet as well as the sp^2 atoms in the chains.[43,45] These two modes were used for subsequent adsorption analysis.

Solvent. Benzene (99.5%; Fluka) was used as solvent without further purification. The simplicity of its NIR spectrum in the desired region (just one peak) ensures an accurate evaluation of the solute concentration.

Adsorbent. Iron sheets (99.5%, temper annealed; Advent Research Materials, Ltd., UK) and iron foil (99.5%, temper hard; Advent Research Materials, Ltd., UK) with a typical analysis of [C] 1200, [Mn] 5000, [S] 500, and [P] 500 ppm were used in the study. The surface roughness was found to be 2−5 μm for Fe sheets and 10−30 nm for Fe foil (AFM data). The iron surface was used to model steel surfaces widely found in petroleum production, transportation, and refining. Surface roughness (30 nm vs 5 μm) was found to be of no importance for the adsorption data presented.

2.3. Data Analysis. *Software and Computing*. The AFM and Raman measurements were controlled by NT-MDT's Nova software. MATLAB 2008b (MathWorks, USA) was used for

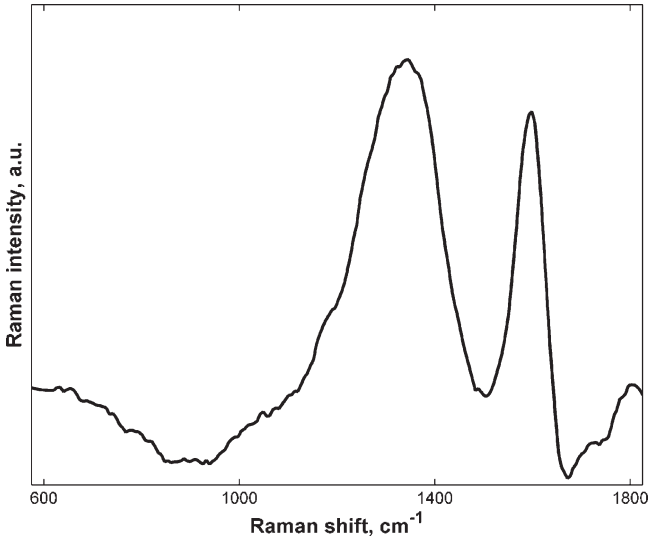

Figure 1. Raman spectrum of asphaltene sample (solid) between 600 and 1800 cm^{-1} after fluorescent background correction. Excitation wavelength: 532 nm; accumulation time: 6 s.

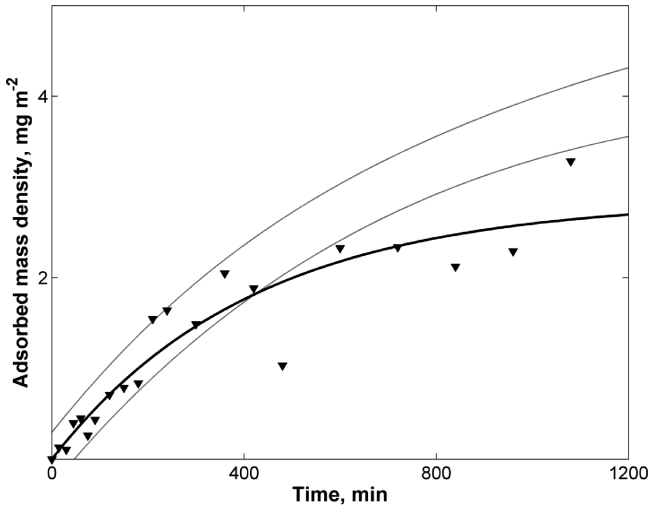

Figure 2. Kinetics of asphaltene adsorption derived from NIR data without PLS analysis. A Langmuir kinetic curve (thick line) is presented. The confidence interval of a PLS curve from Figure 3a (thin lines) is also shown. The difference is due to an incorrect concentration evaluation by the classical method. See text for details.

data analysis. The MATLAB Curve Fitting Toolbox was used for curve fitting. The MATLAB iToolbox was used for building of a partial least-squares (PLS) calibration model.

Concentration Evaluation. Figure 2 presents the results of asphaltene kinetics analysis based on direct evaluation of solution concentration (integral absorption of NIR bands in the 9000−13000 cm^{-1} region). One can see that both the general trend and the data accuracy are unacceptable in this case. Direct spectral analysis without the PLS method leads to lower measured concentration of asphaltenes in benzene solution. This difference becomes greater with increasing solute concentration. The data accuracy (spread of points) also becomes 3−5 times greater if multivariate data analysis is not applied. Effective rate constant ($k_aC_0 + k_d$) of $0.14 \pm 0.07\ h^{-1}$, obtained without partial least-squares regression, should be compared with a value of $0.08 \pm 0.02\ h^{-1}$, evaluated from data in Figure 3a (black curve). Only qualitative estimation of the rate constant is possible due to a 3.8 times greater uncertainty.

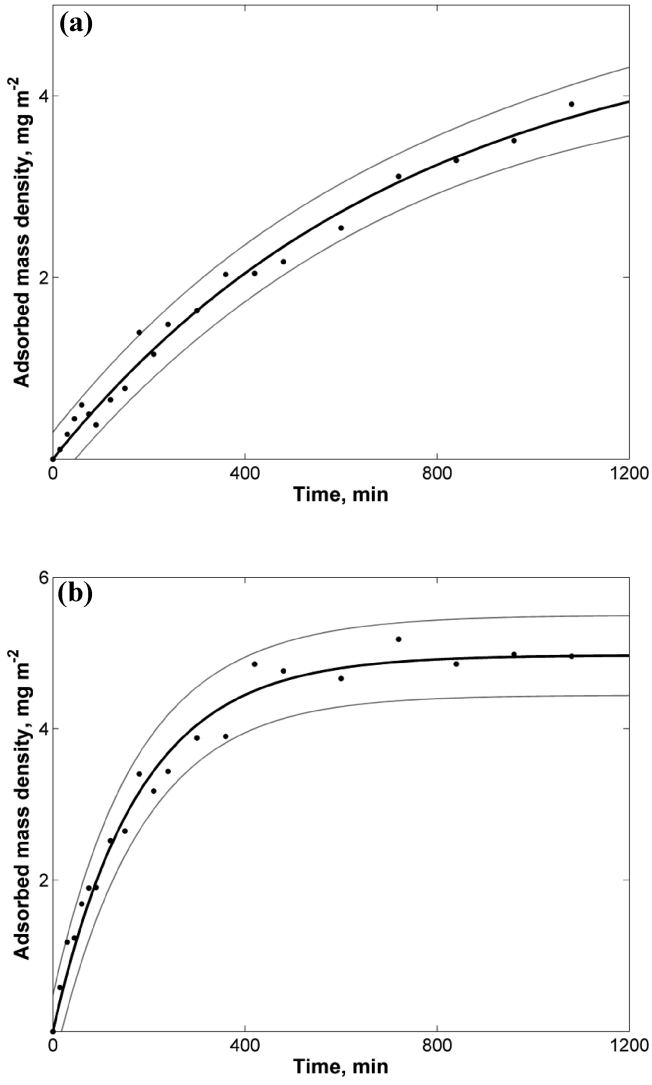

Figure 3. Kinetics of asphaltene adsorption derived from NIR data. Bulk concentration (C_0): (a) 300 and (b) 1250 mg L^{-1}. A fit to a Langmuir model (thick line) with a 95% confidence interval (thin lines) is presented.

Since asphaltenes are a sophisticated mixture of different organic substances with a tendency for aggregation and phase separation,[1,4,8,10,11] their analysis by NIR spectroscopy, which is not a greatly structure sensitive method,[35,39,40] can lead to erroneous conclusions. Fortunately modern mathematics provides us a number of techniques (e.g., PCA, PCR, PLS, etc.)[34,41] specially made for such tasks. Their application greatly improved the informativity of vibrational spectroscopy data.[35,39−42]

The PLS regression method has been used for concentration evaluation from NIR spectroscopic data.[32−36] PLS method finds a linear model by projecting the predicted variables (Y, concentrations) and the observable variables (X, spectra) to a new space. It is used to find the fundamental relations between two matrices (X and Y), i.e., a latent variable approach to modeling the covariance structures in these two spaces. A PLS model will try to find the multidimensional direction in the X space that explains the maximum multidimensional variance direction in the Y space. PLS-regression is particularly suited when the matrix of predictors has more variables than observations, and when there is multicollinearity among X values (e.g., spectral data). The method has proven its efficiency (when compared with classical regression models) in NIR analysis of petroleum resins. See refs 25,37−39 for extra discussion.

Table 3. Parameters of Petroleum Asphaltene Adsorption onto an Iron (Fe) Surface: Langmuir Model

	measured		calculated		
technique	Γ_{max} [mg m^{-2}]	K [L mg^{-1}]	$k_{ads} \times 10^6$ [L mg^{-1} min^{-1}]	$k_{des} \times 10^6$ [min^{-1}]	$-\Delta G_{ads}$ [kJ mol^{-1}]
near infrared (NIR) spectroscopy	4.90 ± 0.07	0.084 ± 0.007	4.95 ± 0.06	59.2 ± 0.2	34.3 ± 0.2
Raman microscopy	5.3 ± 0.5	0.04 ± 0.02	-	-	31.8 ± 1.3

The PLS model has been built using 51 spectra of asphaltene solutions with concentrations from 0 to 1500 mg/L (±0.05 mg/L). The resulting model (3 latent variables[25,32,34,39]) has an accuracy (root mean squared error of prediction, RMSEP) of 0.072 mg/L. All experiments were conducted three times.

Adsorbed Mass Density. The adsorbed mass density $\Gamma(t)$ was evaluated from concentration $C(t)$ according to eq 1

$$\Gamma(t) = \frac{v_0}{s_{ads}}[C_0 - C(t)] \quad (1)$$

where S_{ads} is the total surface area of adsorbent and V_0 is the volume of solution in the cell.

Adsorption Model. A first-order Langmuir adsorption model was applied:

$$\Gamma(t) = \Gamma_{max}\frac{KC_0}{KC_0 + 1}(1 - \exp[-(k_a C_0 + k_d)t]) \quad (2)$$

where Γ_{max} is the maximal adsorbed mass density; $K = k_a/k_d$ is the adsorption equilibrium constant; k_a and k_d are the rate constants of adsorption and desorption, respectively. Equation 2 should be compared with the zero-order model used for petroleum resins adsorption.[25] A detailed derivation of eq 2 can be found in ref 3 and references therein. The parameters of a first-order Langmuir model for asphaltene adsorption should be regarded as effective ones.

Accuracy. Ninety-five percent (95%) confidence intervals are reported (if not specified otherwise).

3. Results and Discussion

3.1. Adsorption Kinetics: Near Infrared (NIR) Spectroscopy Data. Figure 3 shows the adsorption kinetics of petroleum asphaltenes derived from the near-infrared (NIR) spectroscopy data. It is easily seen that asphaltenes reach a stationary mass density value (reaching a plateau) in 200−700 min (3−11 h). The 2 orders of magnitude difference with petroleum resins can be explained by the difference in adsorbent (quartz sand vs iron) and adsorbate structure (rather small molecules vs large polyaromatic ones[3]). Asphaltene dimerization and cluster formation can also influence their adsorption behavior. We have not found any evidence of structural changes (dimerization,[8] oligomerization,[8] selective adsorption,[3] etc.) during the adsorption process or the solute concentration increase. Because vibrational spectra of all samples at all concentrations were rather similar, one can conclude that no great structural changes were observed in the experimental parameter range/during adsorption process. But one should note that NIR spectra are not greatly sensitive to molecular structure, i.e., small changes may be indistinguishable.

Figure 3 shows that even though native asphaltenes are a mixture of many different molecules, their adsorption behavior can be approximated by very simple Langmuir (exponential) kinetics. Of course, the parameters of such a model should be regarded as effective ones.

Comparison of Figure 3a and b clearly shows the concentration dependence of the asphaltene adsorption kinetics (compare with data from ref 3). Extrapolation of the data leads to the conclusion that extremely high asphaltene concentrations would be needed to make these two velocities comparable. Unfortunately, very high asphaltene concentrations render adsorption experiment extremely challenging, due to high light scattering and aggregate formation.[8,25] These results show that formation of asphaltene−resin−paraffin deposition is a multistep process. Of course, in a crude oil, the interaction among different components can alter the adsorption parameters and system behavior.

Table 3 summarizes the kinetic and thermodynamic data obtained in this study. Comparison of adsorption parameters for the resins/quartz[25] and asphaltenes/iron systems leads to a number of interesting conclusions: (i) a much greater value of Γ_{max} is observed for petroleum resins (105 ± 4 mg m^{-2});[25] (ii) an order of magnitude difference in the Gibbs free energy (-34.3 ± 0.2 vs -4.4 ± 0.4 kJ mol^{-1} for resins) means a very high affinity of asphaltene molecules to the steel surface;[25] (iii) the time scale of asphaltene adsorption is 2 orders of magnitude greater.[25] Note also that petroleum resin adsorption is described by zero-order kinetics,[25] in contrast to asphaltene. Further research, focused on the resins/iron system, is needed to clarify the observed differences. Differences in chemical structure most probably affect the adsorption behavior of asphaltenes as compared to petroleum resins. The larger aromatic core in asphaltene molecules, when compared to petroleum resins, can render them more stable in aromatic solution. Together with their higher tendency to aggregate, the Γ_{max} of asphaltanes should be lower than that of resins. An alternative explanation can be found in the fact that asphaltenes do not cover the whole metal surface, but tend to form large aggregates (see below). Finally, the nature of the solvent (benzene, toluene, pyridine, etc.) is very important for any adsorption study.[52,53] Both the adsorption parameters and the adsorbate structure at the Fe surface are dependent on the solvent used.[52,53]

3.2. Adsorption Isotherm: Near Infrared (NIR) Spectroscopy Data. The adsorption isotherm derived from the NIR spectroscopy data is presented in Figure 4. A Langmuir model was fitted to the data. The maximum adsorption mass density (Γ_{max}) and the adsorption constant (K) have been evaluated as 4.90 ± 0.07 mg m^{-2} and 0.084 ± 0.007 L mg^{-1}, respectively (Table 3).

The adsorption mass density reaches its maximum value at a concentration of approximately 250−350 mg L^{-1}. The structure of asphaltenes in this concentration range is not 100% clear,[3,48−51] but one can definitely say that asphaltenes are not "single molecules" but at least (nano)aggregates under these experimental conditions.[48−51] So, the adsorption occurs not from molecular level but from already partly aggregated molecules.

3.3. Raman Microscopy Data. To confirm the kinetic and thermodynamic data presented in Sections 3.1 and 3.2, micro-Raman spectra of metal surfaces after asphaltene adsorption were recorded. Since the Raman intensity is

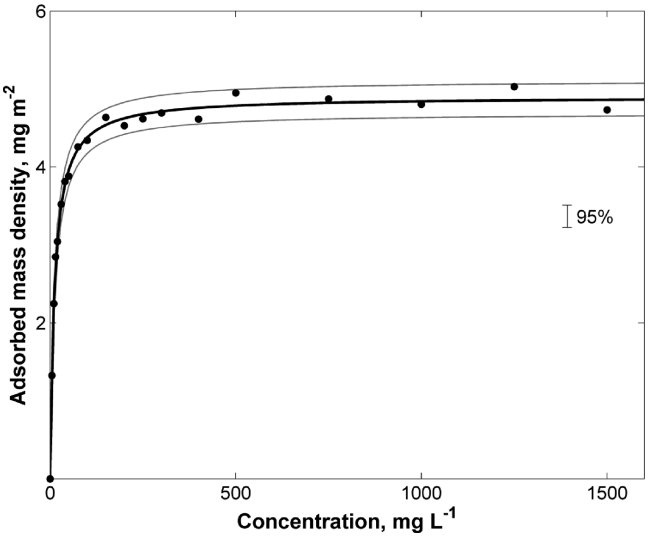

Figure 4. Asphaltene adsorption isotherm derived from NIR data. A Langmuir isotherm (thick line) with 95% confidence interval (thin lines) is presented. The average 95% confidence interval around the data points is also shown.

expected to be proportional to the amount of asphaltenes adsorbed, the Raman measurement can provide us with information about the adsorbed mass density directly.

Raman spectra of adsorbed asphaltenes are very close to solid-state data (see Figure 1). All main Raman features are present in spectra of adsorbed layers. The spectral area under the 1000−1800 cm^{-1} Raman bands (G and the D1 modes,[43−45] see above) was used for calculating the amount of adsorbed asphaltenes. Note that the Raman cross-section was obtained using one NIR data point for normalization (see Section 2).[42]

Results from the Raman experiments are presented in Figure 5a,b and Figure 6. One can see that the Raman data confirm the NIR data. Almost identical behavior of the kinetic curves and the isotherm is observed. Raman microscopy is greatly influenced by the roughness (~3 μm) of the Fe surface, which leads to a greater deviation of individual data points.

3.4. Atomic Force Microscopy (AFM) Data. Atomic force microscopy (AFM) is a unique technique that can provide researchers with rapid and precise information about the topography of surfaces at a scale below 100 nm. Applying AFM to adsorbed layers of asphaltenes results in direct information about structures that are formed by petroleum macromolecules on the metal surface.

Figure 7 shows an example of an AFM image measured on a dry iron surface after asphaltene adsorption. One can see a number of round-elliptical structures (Ø ~200 nm, with a wide size distribution) formed by asphaltenes. They were not observed on an "asphaltene-free" surface, even after contact with benzene. The height of these features is ~50 nm. Thus one can conclude that asphaltenes do not produce a homogeneous molecular layer but rather tend to form aggregates. This behavior can easily be understood if the aggregation tendency of asphaltenes is taken into account. The AFM results of Syunyaev et al.[3] on nonmetallic surfaces (quartz, dolomite, and mica sands) are almost identical to ours, i.e., formation of structures with dimensions of a few hundred nanometers seems to be a general feature of asphaltene adsorption. Further research is needed to confirm this conclusion.

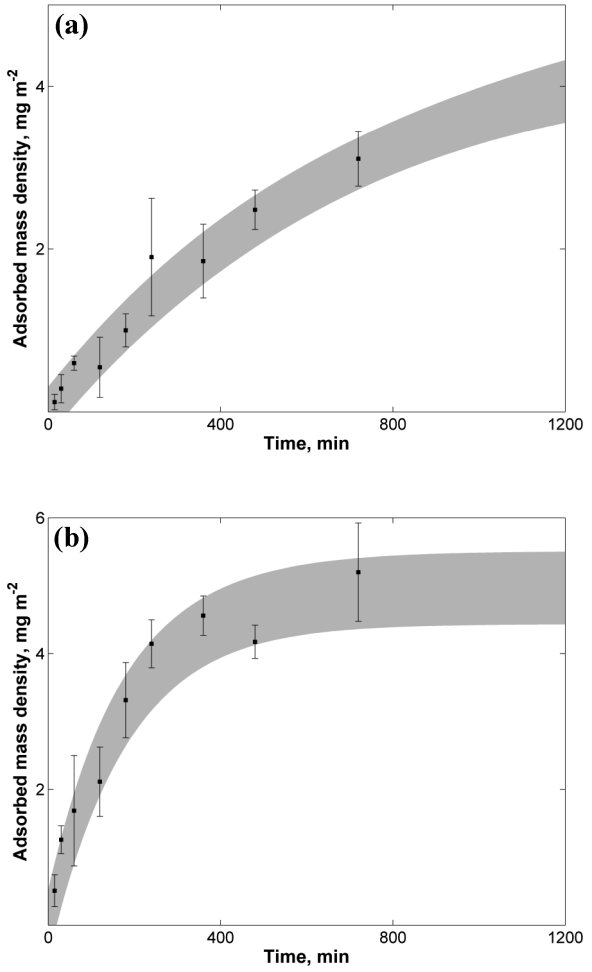

Figure 5. Kinetics of asphaltene adsorption derived from Raman microscopy data. Bulk concentration (C_0): (a) 300 and (b) 1250 mg L^{-1}. The confidence interval of a NIR curve from Figure 3 (gray area) is shown. One NIR adsorption point (60 min) was used for kinetic curve normalization.

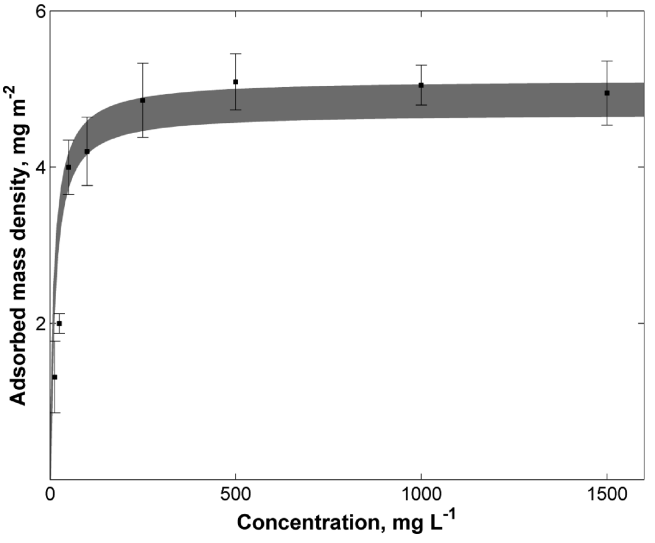

Figure 6. Asphaltene adsorption isotherm derived from Raman microscopy data. The confidence interval of a NIR curve from Figure 4 (gray area) is shown.

Note, however, the use of powders in the corresponding kinetic measurements by Syunyaev et al. on nonmetallic surfaces,[3]

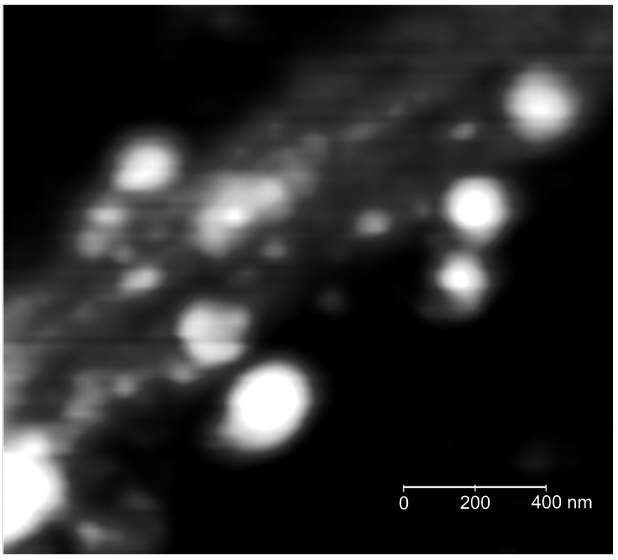

Figure 7. AFM image of iron foil after asphaltene adsorption. *Z*-scale: 63 nm. Bulk concentration is 300 mg L^{-1}; adsorption time is 48 h. AFM data before asphaltene adsorption do not show any of the features displayed in this figure.

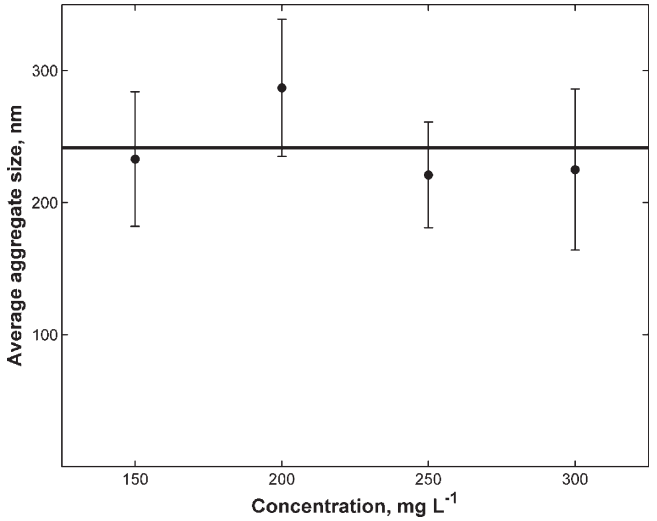

Figure 8. Size dependence of asphaltene aggregates on an iron surface according to AFM data (mean ± sd). At least 350 aggregates were used for averaging. The average value (all four concentrations; black line) is shown.

which renders the kinetic data diffusion-dependent. This was not observed in the current study, due to the use of a flat iron surface.[3,4]

In Figure 8, the dependence of the asphaltene aggregate size on the initial macromolecule concentration in solution is presented. At least in the measured concentration range, the average size of asphaltene aggregates is not significantly affected by the initial bulk concentration. Thus the growth of the adsorbed amount seems to be due to a higher number of asphaltene aggregates, and not because of their growth in size. Of course, such a heterogeneous (colloid) structure of the adsorbed layer is incompatible with the adsorption model, introduced by Langmuir, but since eq 2 correctly describes the adsorption process in the asphaltenes/iron system, one can claim that an "effective" Langmuir-type (exponential) behavior is observed for this system. The parameters fitted should be regarded as "effective" values as shown in ref 54 and references therein.

3.5. Comparison with Previously Published Asphaltene Data. In 2009, Rudrake et al.[2] published a value of -26.8 ± 0.1 kJ mol^{-1} for the Gibbs energy and 9.8 mg m^{-2} for the maximum adsorbed mass density for asphaltene adsorption on gold, using X-ray photoelectron spectroscopy and a quartz crystal microbalance (QCM) method.

Alboudwarej et al.[29] have given values of −37.8, −36.6, and −34.9 kJ mol^{-1} for the Gibbs energy of asphaltene adsorption onto stainless steel (304 L), iron, and aluminum, respectively, based on UV−vis spectrophotometry measurements. Values of 2.70, 1.35, and 0.45 mg m^{-2} for the maximum adsorbed mass density have been reported in the same study.[29] Note that toluene was used as solvent in all cases[2,29] and iron powder with the average particle diameter below 40 μm was used.

Comparison with the results of Alboudwarej et al.[29] shows that our data on the Gibbs energy (equilibrium constant) are very close (-34.3 ± 0.2 vs -36.6 ± 1.5 kJ mol^{-1}),[46] but that the maximum adsorbed mass density values are different (4.90 ± 0.07 vs 1.3 ± 0.5 mg m^{-2}). Two things should be taken into account when comparing these data: (1) the different solvents; (2) the use of iron powder in ref 29. Even though both solvents have approximately the same dielectric constant (∼2.3[47]) their structural difference can influence the results. More serious is the fact that the lower adsorbed mass density has been obtained by using fine iron powder. The general influence of a dispersed structure of the adsorbent (pore diameter, in particular) has recently been shown by Syunyaev et al.[3] One should be very careful when analyzing results of adsorption experiments from colloid adsorbents, as diffusion effects can significantly alter the results.[3,50]

Comparison of the maximum adsorbed mass densities is much more straightforward, as the molecular weight is not needed in this case. This is not true for the Gibbs free energy and other thermodynamic parameters (ΔH, ΔS, etc.). In this case the results are greatly dependent on the choice of MW.[2] Because there is still no agreement between different authors about asphaltene's molecular weight,[5,6] these values should be considered with caution (see also above). The polydispersity of asphaltenes can also play a role in their adsorption behavior. Note that the model for asphaltene adsorption has recently been proposed by Syunyaev et al.[3] and Sjoblom and co-workers.[30]

Kinetic parameters of asphaltene adsorption have not been evaluated in any of the papers discussed above. The values at thermodynamic equilibrium are usually reported. Rudrake et al.[2] found a diffusion-controlled regime in asphaltenes adsorption onto an Au surface. Their time-scale is close to that of Syunyaev et al.[3] and the present research (∼3 h). No obvious concentration dependence of the data of Rudrake et al.[2] can be observed (see Figure 1 in ref 2).

Even though the findings of different studies of asphaltene adsorption agree in general, they differ in the details. More systematic studies will clarify the reasons for the differences found. The major topics that will need to be addressed are (i) the influence of hydrophobicity of the different surfaces (iron, quartz, gold, etc.) and (ii) the influence of the chemical nature of the surfaces. Because all thermodynamic data measured to date show that physical adsorption of asphaltenes from solution takes place, one would expect the physical parameters of the adsorbent (surface) to be of

greater importance than its exact chemical nature. This means that one can hope to build a realistic physical model of asphaltene adsorption onto different industrially important surfaces (e.g., metals and alloys).

According to the thermodynamic data presented, the asphaltene adsorption mass density reaches its maximum values at 250−350 mg L^{-1}. Current literature suggests that asphaltenes form suspended nanoaggregates in this concentration range.[56] It can be proposed that with an increase of the asphaltene concentration above 250 mg L^{-1}, aggregation in bulk becomes the energetically favorable process for petroleum macromolecules, while the adsorption process slows down. The adsorbent surface would then saturate with nanosize aggregates (see AFM data). Any further increase of the solution concentration leads to "structuring" of solution asphaltenes (growth in particle size and aggregation of nanoparticles).[1,4]

4. Conclusions

The following conclusions are drawn:

(1) Combining near-infrared (NIR) spectroscopy, Raman microscopy, and atomic force microscopy (AFM) was found to produce full and consistent information about the asphaltene adsorption process.

(2) The Gibbs energy of asphaltene adsorption onto iron was found to be -34.3 ± 0.2 kJ mol^{-1}; the adsorption and desorption rate constants were measured to be $(4.95 \pm 0.06) \times 10^{-6}$ L mg^{-1} min^{-1} and $(59.2 \pm 0.2) \times 10^{-6}$ min^{-1}, respectively. These values were confirmed by Raman microscopy (Table 3).

(3) Asphaltenes were found to form aggregates on the iron surface with a few hundred nanometers diameter and approximately 50 nm high. No clear concentration dependence of the aggregate size was observed.

(4) The conclusions of Sjöblom and co-workers[30] about the nonuniform distribution of petroleum macromolecule on metal surfaces have been confirmed.

(5) Even if a Langmuir-type dependence of the absorbed mass on the asphaltene concentration is observed, multilayer adsorption is possible.

Although a number of studies, including the current work, have reported Langmiur-type adsorption of asphaltenes on a variety of surfaces, the parameters of the Langmuir model should be regarded as effective parameters (see ref 54 and references therein). These works were done with diluted samples (see Section 3.4).

It should eventually be possible to find a relationship between the asphaltene surface excess (adsorbed mass density) and the aggregate size in solution, and to take many experimental parameters (concentration, temperature, pressure, solvent type, etc.) into account. Further research will be needed to derive such a relationship. Additional adsorption data are also needed to clarify whether resins adsorb onto metal surfaces and if other petroleum macromolecules create full asphaltene−resins−wax (asphaltene−resins−paraffin) deposit.[1,4] Considering the high chemical information content of vibrational spectroscopy data, near-IR spectroscopy and Raman microscopy are attractive techniques for the modern petroleum science and industry.